Remote Sensing

Article

Riding Quality Model for Asphalt Pavement Monitoring Using Phase Array Type L-band Synthetic Aperture Radar (PALSAR)

Weerakaset Suanpaga * and Kamiya Yoshikazu

Remote Sensing and Geographic Information Systems Field of Study, School of Engineering and Technology, Asian Institute of Technology, Thailand; E-Mail: kamiya@ait.ac.th

* Author to whom correspondence should be addressed; E-Mail: weerakaset@gmail.com; Tel.: +66-81-950-0085; Fax: +66-2-579-7565.

Abstract: There are difficulties associated with near-real time or frequent pavement monitoring, because it is time consuming and costly. This study aimed to develop a binary logit model for the evaluation of highway riding quality, which could be used to monitor pavement conditions. The model was applied to investigate the influence of backscattering values of Phase Array type L-band Synthetic Aperture Radar (PALSAR). Training data obtained during 3–7 May 2007 was used in the development process, together with actual international roughness index (IRI) values collected along a highway in Ayutthaya province, Thailand. The analysis showed that an increase in the backscattering value in the HH or the VV polarization indicated the poor condition of the pavement surface and, of the two, the HH polarization is more suitable for developing riding quality evaluation. The model developed was applied to analyze highway number 3467, to demonstrate its capability. It was found that the assessment accuracy of the prediction of the highway level of service was 97.00%. This is a preliminary study of the proposed technique and more intensive investigation must be carried out using ALOS/PALSAR images in various seasons.

1. Introduction

Nowadays, natural disasters are becoming more frequent and more destructive. In particular, their effects on highway pavements cannot be monitored quickly or in near-real time. Currently, researchers are concerned with methods of monitoring pavement conditions. Failure of the pavement can be categorized into two types: structural failure and functional failure. The inspection methods that can be used to identify the type of damage, can be separated into four conditions: structural, distress or surface, safety or skid resistance and roughness. The structural condition can report on structural failure and the last three conditions report on functional failure. The engineer's task is to design a safe, man-made structure, using design standards to avoid structural failure of any man-made components. While pavement structure is one type of man-made structure, the pavement life may be damaged primarily by functional failure. The assessment of condition, in terms of functional failure in the existing pavement, is essential for any land transportation program. In a developed country (e.g., the U.S.), much of the current investment has been in pavement maintenance and rehabilitation, rather than in new construction [1].

The international roughness index (IRI) is used to evaluate new and rehabilitated pavement conditions and for construction quality control/quality assurance purposes [2]. It can be used also to summarize the roughness qualities that impact vehicle response and is most appropriate when a roughness measure is desired that relates to the overall vehicle operating cost, ride quality and surface condition [3]. Roughness measurements are usually expressed in terms of meters per kilometer (m/km) or millimeters per meter (mm/m). The IRI is based on the average rectified slope (ARS), which is a filtered ratio of a standard vehicle's accumulated suspension motion (in mm, inches, *etc*.) divided by the distance traveled by the vehicle during the measurement (km, miles, *etc*.). The IRI is then equal to the ARS multiplied by 1,000. Roughness (IRI) relates to the initial IRI, the percentage of fatigue cracking and the average rut depth [4]. The IRI is the index most widely used for representing pavement roughness. ASTM E 1926 defines the standard procedure for computing the IRI from longitudinal profile measurements based upon a mathematical model, referred to as a quarter-car model. The quarter-car is moved along the longitudinal profile at a simulation speed of 80 km/h and the suspension deflection is calculated using the measured profile displacement and standard car structure parameters. The simulated suspension motion is accumulated and then divided by the distance travelled to give an index with a unit of slope (m/km).

Surveys of state highway agencies in the United States indicated that about 10% (4 out of 34 respondents) used the IRI to control initial roughness [5], while about 84% (31 out of 37 respondents) used the IRI to monitor pavement roughness over time [6], making it the statistic of choice for roughness specifications. The proposed 2002 Design Guide under development by the National Cooperative Highway Research Program (NCHRP) proposed also to include IRI prediction models that are a function of the initial IRI (IRI0) [5,7].

Many techniques using a geographic information system (GIS) have been developed to determine pavement quality [1,5,8-11]. In particular, the real-time data of highway pavement conditions were recorded from highway service vehicles (IVECO Daily) [12]. The system was developed by Autostrada del Brennero S.p.A and was capable of capturing temperature data in all lanes and providing real-time storage to a central GIS acting as a map server. This system was also the first to

support a winter maintenance service system to rate and improve the construction quality and resultant increase in the life cycle of the road pavement. The ground penetrating radar (GPR) was applied to evaluate existing highways in Scandinavia by identifying soil type, thickness of overburden, compressibility and frost susceptibility of the sub-grade soil, as well as measuring layer thickness and subsurface defects using GPR [13]. Many authors have worked on the evaluation of existing highways by remote sensing and GIS. The airborne laser [14] and swath mapping technology [15] were used for coastal and highway mapping in Florida. In another study, the LIDAR-based elevation data was used to evaluate the highway condition [16]. However, such methods are costly.

The timing of maintenance and rehabilitation actions can greatly influence their effectiveness and cost, as well as the overall pavement life. Figure 1 shows that for the first 75% of pavement life, the pavement condition drops by about 40%. However, it only takes another 17% of pavement life for the pavement condition to drop another 40% [17]. Additionally, it will cost four to five times as much if the pavement is allowed to deteriorate for even two to three years beyond the optimum rehabilitation point. The cost increase is caused by: (1) the pavement condition must be improved by a greater amount (for example, from "very poor" to "very good" *versus* from "fair" to "very good"); and (2) it costs more money per unit of pavement condition increase (it costs more to go from "very poor" to "poor" than it does from "fair" to "good"). Thus, if it were possible to reduce the cost and monitor the highway pavement more frequently, there would be several benefits. At present, developing a model using microwave remote sensing technology is a new option to evaluate pavement condition in real or near-real time, because the revisit day of the satellite to the same place is every 46 days, or eight times per year, which can greatly influence the model effectiveness and impact favorably on the cost, as well as the overall pavement life.

Figure 1. Rehabilitation time *versus* cost (adapted from [17]).
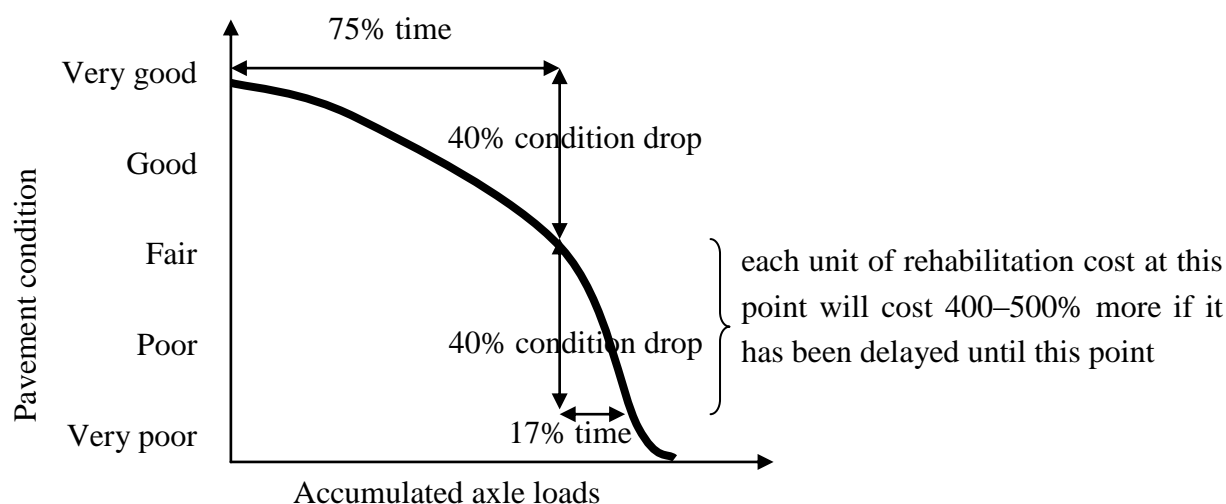
1.1. ALOS Characteristics

The Advanced Land Observing Satellite (ALOS) was launched into a sun-synchronous orbit on 24 January 2006 under a joint project of the Ministry of Economy, Trade and Industry (METI) and the Japan Aerospace Exploration Agency (JAXA). With its orbit at an altitude of 691.65 km and 98.16°

inclination, ALOS revolves around the earth every 100 minutes, or 14 times each day and repeats its path (repeat cycle) every 46 days. The ALOS has three payloads: the panchromatic remote sensing instrument for stereo mapping (PRISM), the advanced visible and near infrared radiometer type 2 (AVNIR-2), and the phased array type L-band synthetic aperture radar (PALSAR) [18]. Details of the system are shown in Table A1 in the appendix.

1.2. PALSAR Characteristics

PALSAR is an active microwave radar using the L-band frequency to achieve cloud-free and day-and-night land observation. It has three modes, namely high resolution, ScanSAR, and polarimetric mode. The high resolution mode is used under regular operation and it has a ground resolution of 7 m. The ScanSAR mode enables the off-nadir angle to be switched from three to five times (scanning a swath of 70 km) to cover a wide area from 210 km^2 (70 $\times$ 3) to 350 km^2 (70 $\times$ 5), but the resolution is inferior to that of the high resolution mode. PALSAR can simultaneously receive both horizontal (H) and vertical (V) polarization per each H and V polarized transmission, called multi polarimetry or full polarimetry (HH, HV, VH and VV polarization). The incidence angle ranges from 8 to 30 °. This polarimetric mode was used in the current study.

1.3. Highway Riding Quality (HRQ)

Highway riding quality is seen as a quantitative indicator of the riding conditions of a highway and of the user's perception of this condition [19].

1.4. Levels of Highway Riding Service (LHR)

Levels of highway riding service are qualitative indicators that characterize the riding conditions of a highway, and the user's perception of these conditions. In contrast, highway riding quality is *quantitative* [19].

1.5. Determinants (DTMs)

HRQ can be measured by one or several determinants. The selection of determinants or factors should describe the riding quality and also reflect drivers' perception.

The relationship among the LHR, HRQ and DTMs, which have identified that LHR are determined by selecting HRQ as quantified by selected measurements of DTMs. LHR is separated into four word designations (fair to excellent) , with "fair" describing the lowest range of quality and "excellent" describing the highest range of quality.

1.6. Objectives

The objective of the study was to examine whether the backscattering data of ALOS/PALSAR could be related with the international roughness index (IRI) data and to develop a multinomial logit model for the evaluation of level of highway riding service.

2. Study Area

Phra Nakhon Si Ayutthaya or the Ayutthaya province is located in central Thailand (Figure 2). Highways that are the responsibility of the Department of Highways (DOH) in the Ayuthaya province are shown in Figure 3. The province has a total area of 2,546.35 km^2 and the neighboring provinces are (from north clockwise): Ang Thong, Lop Buri, Saraburi, Pathum Thani, Nonthaburi, Nakhon Pathom and Suphan Buri. The Ayutthaya province is located in the flat river plain of the Chaophraya River valley and is surrounded by the Lop Buri and Pa Sak rivers. Rice farming is the main occupation in the area, involving 769,126 people in 2008, over an area of 779.2 km^2. The study site is at latitude 14°20′58″N and longitude 100°33′34″E, which equates to WGS84 format as UTM Zone 47 at 14.349444N, 100.559444E.

The highways in the Ayuthaya province total 738.493 km in length. The DOH categorizes the pavement into two types: asphalt cement concrete (ACC) or flexible pavement; and Portland cement concrete (PCC) pavement or rigid pavement. The total length of highways of ACC is 231.897 km and the PCC pavement has a total length of 506.596 km. There are two main highways: (1) highway number 32 is a 6-lane divided highway, 21 m wide, which has a flexible pavement; and (2) highway number 1 is a 10-lane divided highway, 35 m wide, with a PCC pavement [20]. Table 1 shows only the characteristics of the ACC highways sampled that were the responsibility of the Ayutthaya DOH in 2007.

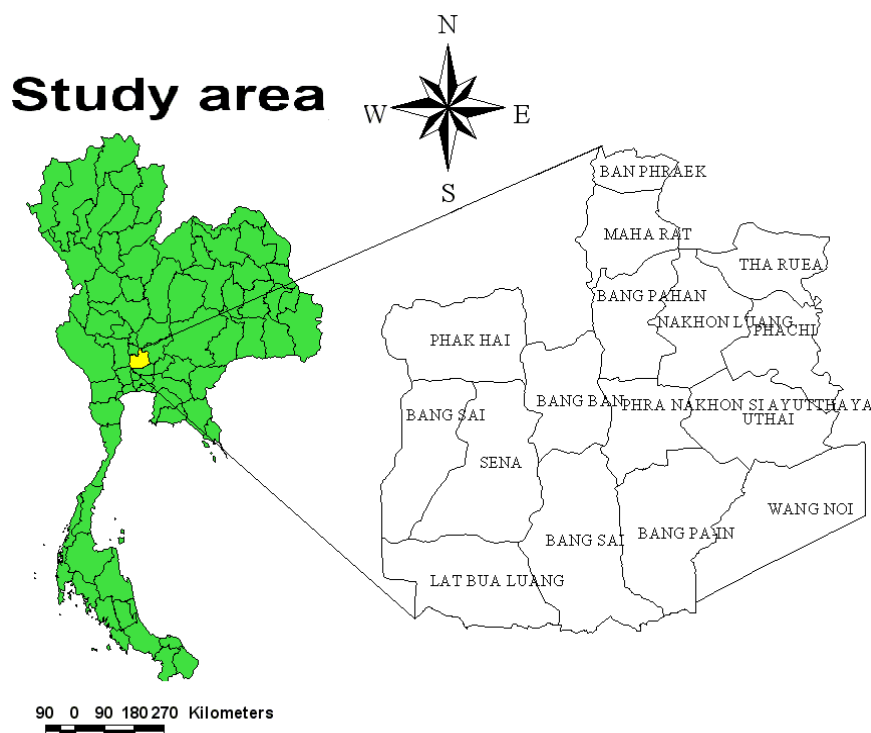**Figure 2.** Location of study area in Ayutthaya province, Thailand.

Figure 3. The highways (blue lines) in Ayutthaya province that are the responsibility of the DOH.
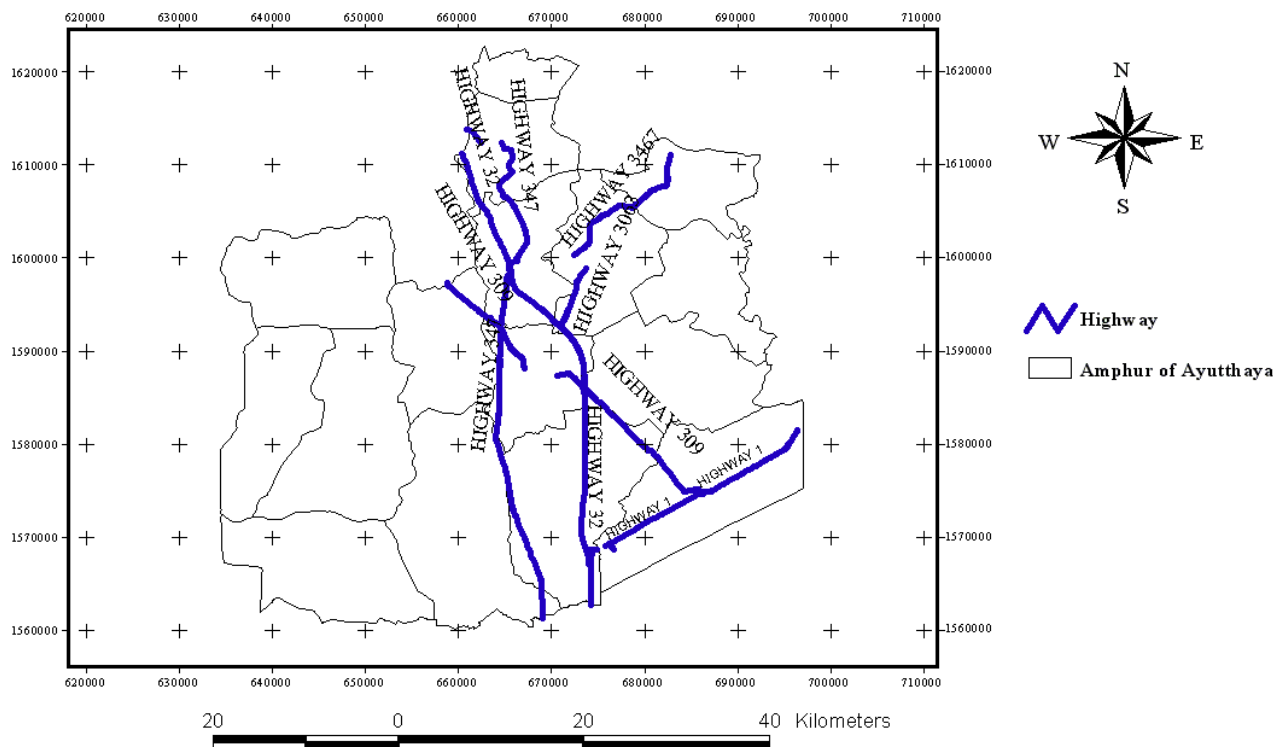

Table 1. Characteristics of the asphalt highways sampled that were the responsibility of the Ayutthaya DOH in 2007.

Highway Number	Distance (km)	Number of Lanes	Divided	Width of Surface Plus Shoulder (m)	IRI Average (mm/m)
32	48.605	6	YES	23	3.59
309	28.608	2–3	NO	8–11.5	2.29
347	44.576	2–3	NO	8–11.5	2.4
3063	9.389	2	NO	8	4.12
3467	19.556	2	NO	8	2.44

3. Method and Data

The level of highway riding service was determined using a multinomial logit (ML) model. Estimation of the parameters of this model can be carried out easily using the ML method. In large samples, these estimates have been proven to have all the usual desirable statistical properties [21]. The dependent variable was the ground-truth IRI data measured by the bump integrator. The DTMs were the backscattering data in four polarizations (HH, HV, VH and VV). The method involved the following steps:

1. Input data preparation: the ground-truth IRI data from DOH and digital readings of backscattering from the PALSAR image.

2. Calculation of the descriptive statistical values of IRI and backscattering data: the maximum, minimum, mean and standard deviation values of the IRI data and backscattering data sampled along the highway were calculated.

3. Building of the utility function of the riding quality choice model (multinomial logit model) from the IRI and backscattering data.

4. Parameter estimation: estimates were obtained using the maximum likelihood method.

5. Goodness of fit test for selection: the backscattering polarization that had the highest McFadden log likelihood ratio index (ρ^2) and the greatest significance by the t-test and sign test was selected to be the most appropriate polarization.

6. Validation of the level of riding service model.

7. Application of the level of the riding service model to highway number 3467.

3.1. Input Data

Backscattering data was collected using an ALOS/PALSAR image resolution of 12.5 m. The single path IRI data was collected from the bump integrator on a moving vehicle as ground-truth data. All highway data was sampled during 3–7 May 2007.

3.2. Backscattering Data

An ALOS/PALSAR scene (ALPSRP067770280-P1.5GUA) was used for analysis with an image resolution of 12.5 m, an image scene center latitude of 14.449 ° and longitude of 100.622 °, (653603.184N, 1633021.952E) and an observation date in UTC of 2007/05/03. Figure 4 shows the back scattering image with HH, HV, VH and VV polarization, overlaid by highways and the Ayutthaya provincial boundary. Table A2, in the Appendix, shows detailed information for the PALSAR sensor. Prior to use in the current study, radiometric calibration had been applied to the PALSAR product at Level 1.5, defined in the PALSAR product specifications by JAXA as normalizing all pixels using the cosine of the incidence angle.

Figure 4. ALOS/PALSAR image (Scene ID: ALPSRP067770280-P1.5GUA), with back scattering in the HH, HV,VH and VV polarization, overlaid with highways (red) and the Ayutthaya provincial boundary (white).
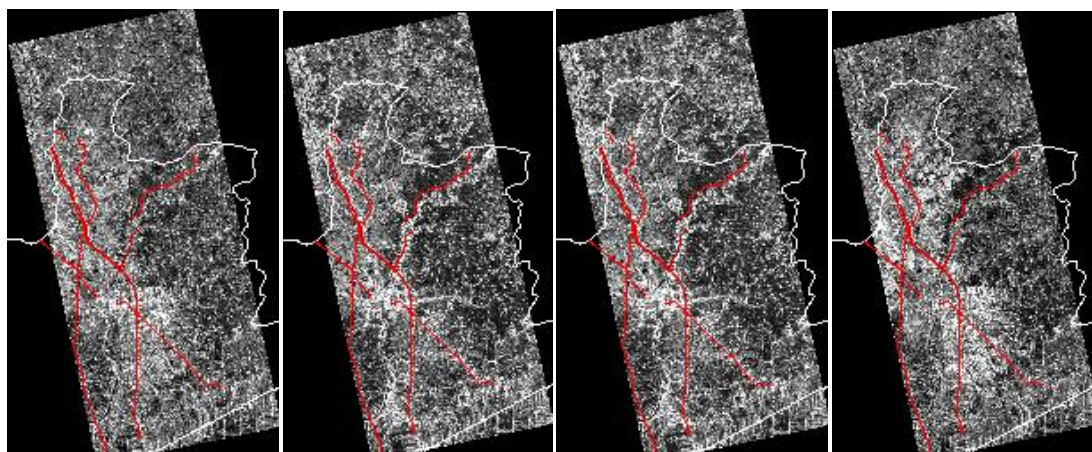
Table 2 shows basic statistics for the whole area of the backscattering values in all directions of polarization .The average backscattering value of the HH polarization was not different from the VV polarization and the average backscattering value of the HV polarization was not different from the VH polarization. For the study area, the average backscattering value and the range in value in the co-polarization plane was higher than in the cross-polarization plane. Table 3 also shows one advantage of the higher range in values, is that there should be a high correlation between co-polarization and the IRI value in the development of a riding quality model.

Table 2. Basic statistics for the whole area of backscattering values in each direction of polarization.

	Backscattering Value (Unit: Digital Number, DN)			
	HH	**HV**	**VH**	**VV**
Average	3,450.7	1,071.9	1,046.4	3,079.8
Standard Deviation	3,434.4	1,038.5	1,006.5	3,112.7
Maximum	65,535	54,410	54,313	65,535
Minimum	257	214	213	257
Number of Pixels	12,083,508	12,083,505	12,083,504	12,083,508

Table 3. Basic statistical values along the ACC highway sampled.

	Backscattering Value (Unit: DN)				IRI (mm/m)
	HH	**HV**	**VH**	**VV**	
Average	4,560.74	1,816.01	1,753.68	4,355.02	3.40
Standard Deviation	1,197.14	549.32	521.24	1,176.29	1.08
Maximum	10,786	3,844	3,569	8,885	9.14
Minimum	2,208	911	829	1,964	2.01
Number of Pixels	400	400	400	400	400

3.3. IRI Data

To classify the level of highway riding service, 400 IRI samples (Table 3) throughout Thailand were classified by the DOH standard and the level of highway riding service was separated into four classes (Table 4) [21].

A low IRI value indicates a very smooth highway surface, while a high IRI value means the highway surface is very rough. The level of riding service was assigned a value ranging from excellent (lowest value) through good and fair to poor (highest value).

**Table 4.** IRI values and associated road surface condition.

IRI (m/km or mm/m)	Level of Highway Riding Service
≤ **2.50**	Excellent
2.5–3.50	Good
3.5–4.50	Fair
> 4.5	Poor

4. Results and Model Explanation

4.1. Multinomial Logit Model

To develop levels for the highway riding service model, firstly, it was necessary to evaluate which backscattering polarization data had the highest correlation with the IRI, so the relationship between the IRI and backscattering value for each set of polarization data was determined. In this study, the backscattering polarizations were the DTMs. Figure 5 shows the relationship between the IRI and backscattering value for each set of polarization data (HH, HV, VH and VV). It was found that the backscattering value with HH polarization had the highest Pearson correlation (r = 0.8293) that was significant at the 0.01 level (two-tailed test). Consequently, this polarization was used as the input parameter in the model.

Figure 5 Relationship between IRI and backscattering values for each set of polarization data: HH (top left), HV (top right), VH (bottom left) and VV (bottom right). Note: ** = correlation significant at the 0.01 level (two-tailed test).
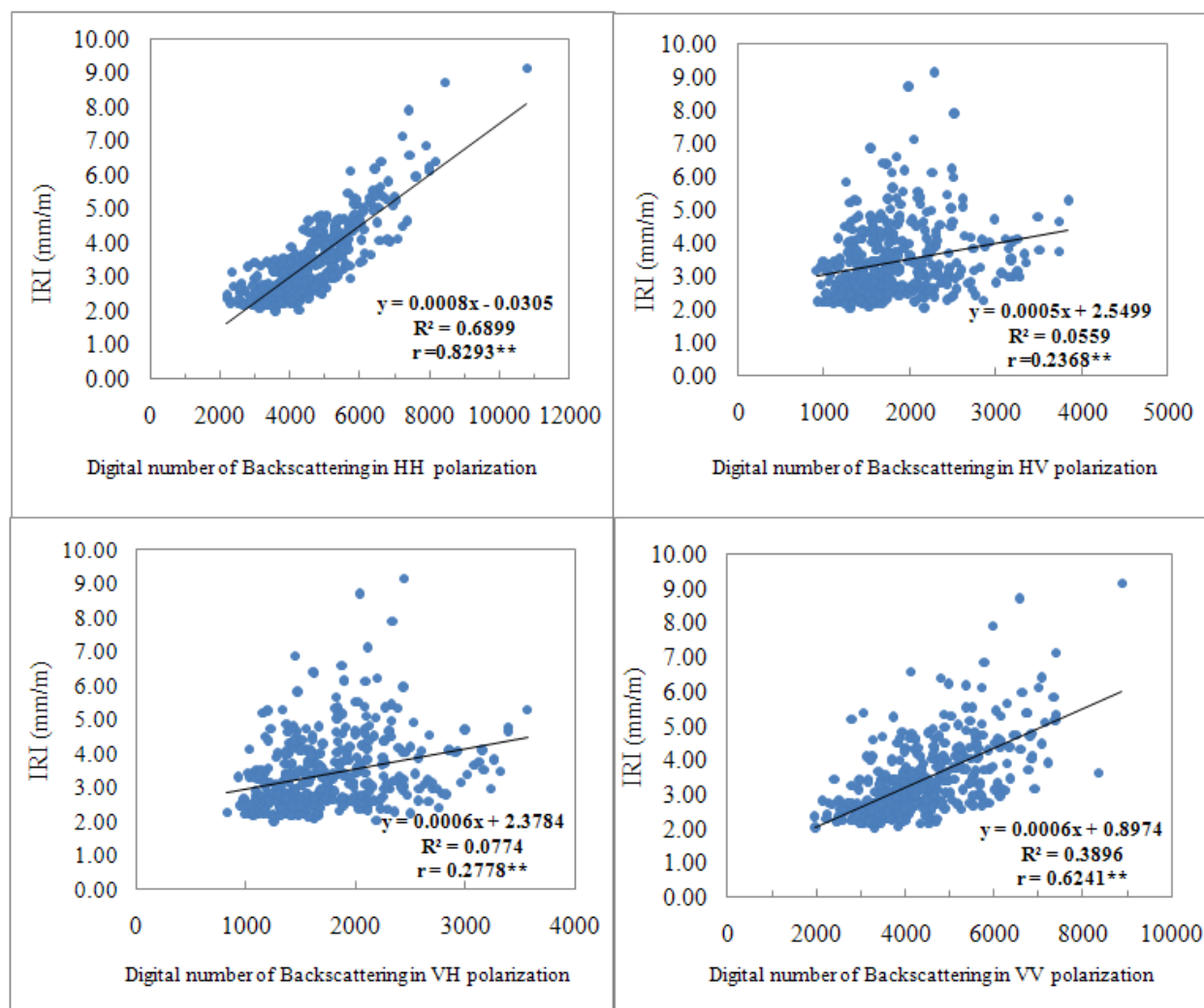
Secondly, to produce the utility function of the riding service model, the IRI dependent data was converted to the level of highway riding service data according to the Thailand-DOH standard

(Table 4). Consequently, the qualities in the riding service estimation model were constructed using Equations 1–3, with the reference category being the poor condition. This model was significant at the 0.01 level (two-tailed test), the global test for the constant variable (β_0) tested the null hypothesis that $\beta_0 = 0$ and variable *DNHH* tested the null hypothesis that *DNHH* = 0. All variables in Equations 1–3 were significant at the 0.01 level with student's *t*-test (two-tail).

$$\text{HRQ}_{\text{fair|poor}} = 8.7302 - 0.0015 DNHH \tag{1}$$
$$(t = 5.40)\ (t = -5.20)$$

$$\text{HRQ}_{\text{good|poor}} = 21.0454 - 0.0039 DNHH \tag{2}$$
$$(t = 9.85)\ (t = -9.65)$$

$$\text{HRQ}_{\text{excellent|poor}} = 25.4662 - 0.0053 DNHH \tag{3}$$
$$(t = 10.99)\ (t = -11.28)$$
$$(\rho^2 = 0.36,\ \chi^2 = 364.86,\ df = 3,\ p = 0.00)$$

where: *DNHH* is the digital number of HH polarization; $\text{HRQ}_{\text{fair|poor}}$ is the highway riding quality of service of the fair condition with reference to the poor condition; $\text{HRQ}_{\text{good|poor}}$ is the highway riding quality of service of the good condition with reference to the poor condition; and $\text{HRQ}_{\text{excellent|poor}}$ is the highway riding quality of service of the excellent condition with reference to the poor condition.

Using the riding quality model developed, it was possible to determine the probability of selecting the level of riding service using Equations 4–6, with the reference category being the poor condition:

$$P_{\text{fair}}(DNHH) = \frac{1}{1 + \exp[-8.7302 + 0.0015\,DNHH]} \tag{4}$$

$$P_{\text{good}}(DNHH) = \frac{1}{1 + \exp[-21.0454 + 0.0039\,DNHH]} \tag{5}$$

$$P_{\text{excellent}}(DNHH) = \frac{1}{1 + \exp[-25.4662 + 0.0053\,DNHH]} \tag{6}$$

The probability of selecting the poor riding service could be determined by using Equation 7:

$$P_{\text{poor}}(DNHH) = 1 - P_{\text{fair}}(DNHH) - P_{\text{good}}(DNHH) - P_{\text{excellent}}(DNHH) \tag{7}$$

The decision criteria to select the level of highway riding service model were provided using Equation 8:

$$LHR = \begin{cases} \text{poor},\ P_{\text{poor}}(DNHH) > P_{\text{fair}}(DNHH), P_{\text{good}}(DNHH), P_{\text{excellent}}(DNHH) \\ \text{fair},\ P_{\text{fair}}(DNHH) > P_{\text{poor}}(DNHH), P_{\text{good}}(DNHH), P_{\text{excellent}}(DNHH) \\ \text{good},\ P_{\text{good}}(DNHH) > P_{\text{poor}}(DNHH), P_{\text{good}}(DNHH), P_{\text{excellent}}(DNHH) \\ \text{excellent},\ P_{\text{excellent}}\ DNHH > P_{\text{poor}}(DNHH), P_{\text{fair}}(DNHH), P_{\text{good}}(DNHH) \end{cases} \tag{8}$$

where: *LHR* is the level of riding service; $P_{\text{poor}}(DNHH)$ is the probability number of HH polarization of the poor condition; $P_{\text{fair}}(DNHH)$ is the probability number of HH polarization of the fair condition; $P_{\text{good}}(DNHH)$ is the probability number of HH polarization of the good condition; and $P_{\text{excellent}}(DNHH)$ is the probability number of HH polarization of the excellent condition.

Table 5 shows the classification results obtained using the level of riding service model (multinomial logit model). Validation of this model indicated that the model was only 61.00% correct. Consequently, a binary logit model was developed.

Table 5. Classification results using the first level of riding quality model (multinomial logit model).

Observed	Predicted				Percent Correct
	Fair	**Poor**	**Good**	**Excellent**	
Fair	32	20	6	0	55.17
Poor	11	46	27	0	54.76
Good	2	19	145	17	79.23
Excellent	0	0	54	21	18.00
Overall percentage	11.25	21.25	58.00	9.50	61.00

4.2. Binary Logit Model

Binary logit model was developed by reclassifying the level of riding service into two groups, namely good, if the IRI value was less than or equal to 3.5 mm/m, otherwise the quality was classified as poor. The new quality of riding service estimation model was constructed as Equation 9. This model was significant at the 0.01 level (two-tailed test), the variable β_0 and variable *DNHH* were significant at the 0.01 level with student's *t*-test (two-tail).

$$\text{HRQ}_{\text{good|poor}} = 14.4799 - 0.0029 \; DNHH \tag{9}$$
$$(t = 9.87) \; (t = -9.69)$$
$$(\rho^2 = 0.54, \; \chi^2 = 279.39, \; df = 1, \; p = 0.00)$$

where: *DNHH* is the digital number of the HH polarization; HRQ $_{\text{good|poor}}$ is the highway riding quality of service of the good condition with the reference category being the poor condition.

Using this riding quality model, the probability to select the level of riding service could be determined as shown in Equation 10 (the reference category is the poor condition). The decision criteria to select the level of highway riding service model were provided using Equation 11:

$$P_{\text{good}} \, (DNHH) \; = \; \frac{1}{1+\exp\left[-14.4799+0.0029 \; DNHH\right]} \tag{10}$$

$$LHR \; = \; \begin{cases} \text{good}, P_{\text{good}} \, (DNHH) \geq 0.50 \\ \text{poor}, P_{\text{good}} \, (DNHH) < 0.50 \end{cases} \tag{11}$$

Table 6 shows validation of the binary logit function, after substitution of the digital number (DN) value into the logit model indicated that the model had an accuracy assessment of prediction of the highway level of service equal to 87.00% (using data from highway numbers 32, 309, 347 and 3063).

Table 6. Classification results using the second level of riding quality model (binary logit model).

Observed	Predicted		Percent Correct
	Poor	**Good**	
Poor	112	30	78.87
Good	22	236	91.47
Overall percentage	33.50	66.50	87.00

The marginal effect of decision criteria to select good riding service was derived from the partial derivative of Equation 10 and was calculated using Equation 12. A unit increase in the DNHH value decreased the probability of selecting the good level by 0.00289.

$$\frac{\partial P_{good}\ (DNHH_i)}{\partial DNHH_i} = 0.0029(\frac{-1}{1+\exp{[-14.4799+0.0029\ DNHH_i]}}) \tag{12}$$

Figure 6 shows the relationship between backscattering and the probability of selection of highway service level being good. From the probability function of the binary logit model, if the DNHH value is greater than or equal to 4,946 (14.2445/0.00288), then the riding service will be poor. With reference to the marginal effect, it was concluded that if the DNHH value increased further, then the level of riding service would become very poor.

Figure 6. Relationship between backscattering and probability of selection of highway service level = good.
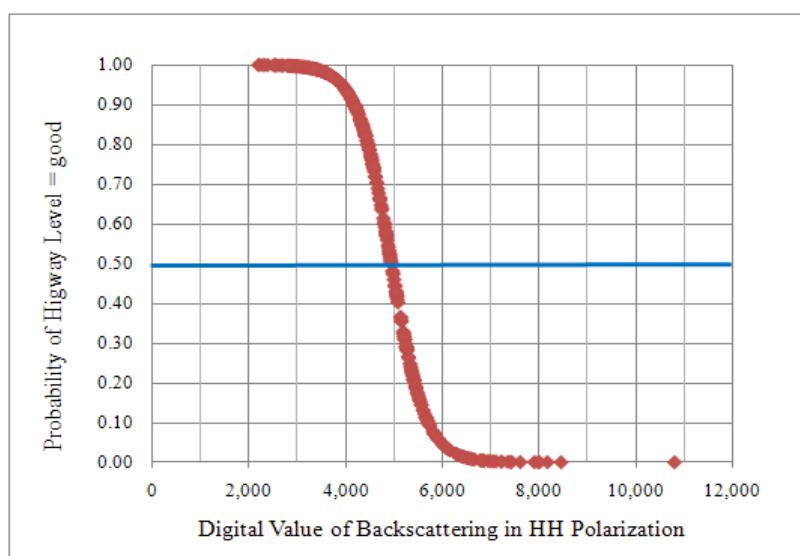
The application of a binary logit model to highway number 3467, involved substitution of the backscattering value (100 samples) into the model for the probability of selecting the good condition, which resulted in the accuracy assessment for the prediction of the highway level of service being 97.00% (Table 7).

Table 7. Classification results using the level of riding quality model of highway number 3467 (100 samples).

Observed	Predicted		Percent Correct
	Poor	**Good**	
Poor	12	2	85.71
Good	1	85	1.16
Overall percentage	12.00	85.00	97.00

Figure 7 shows the relationship between backscattering and the probability of selection of highway number 3467 with service level equal to good. It can be concluded that if the

backscattering value is approximately more than 5,000, then the level of pavement service will be poor.

Figure 7. Relationship between backscattering and the probability of selecting highway number 3467 with service level = good.
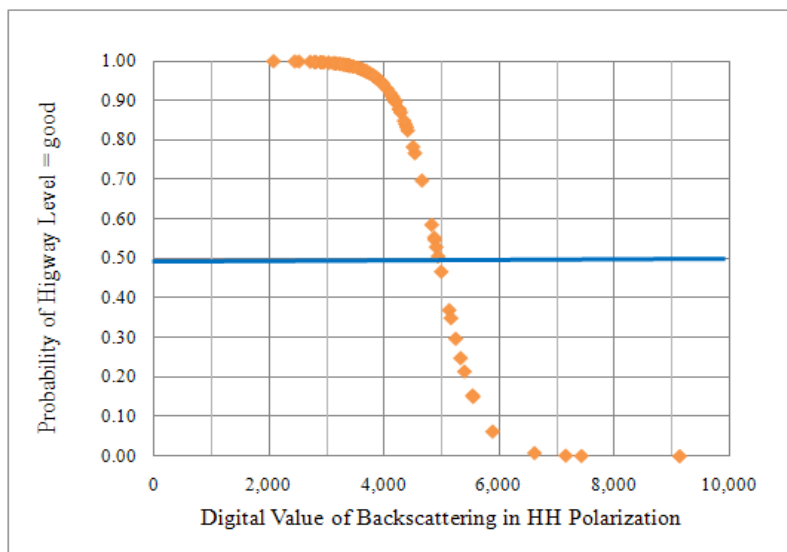
5. Discussion and Conclusion

A new approach was proposed to determine the level of highway riding service using the binary logit model. After the back substitution of DNHH in this function, the accuracy of the approach was 87.00%. The analysis showed that an increase in the backscattering value for copolarization, in either the HH or VV polarization, indicated a poor condition of the pavement surface. It was concluded that the most suitable variable for developing riding quality evaluation was the backscattering value of the HH polarization. From the probability function of the binary logit model, if the DNHH value were greater than or equal to 4,946 (14.2445/0.00288), then the riding quality would be poor. From the marginal effect function of the binary logit model, if the DNHH value were to increase further, then the level of riding service would become very poor. The models developed were applied to analyze highway number 3467 (100 samples) to demonstrate the capability of each model. It was found that the accuracy assessment for the prediction of the highway level of service equaled 97.00%.

Since only one set of ALOS/PALSAR images (during 3–7 May 2007) was used in this study, and as this is a preliminary study of the proposed technique, more intensive investigation must be carried out using ALOS/PALSAR images in various seasons.

In future, satellite data resolution may be finer than 12.50 m, for example, down to a resolution of 3 m, so that the accuracy would be greater than in this analysis and an automatic technique could be applied. Because the PALSAR resolution was only 12.5 m and the IRI data, on average, was only about 25.0 m, the current study used an average of two pixels of PALSAR resolution. In further studies, it should be possible to record the IRI value to be less than or equal to the PALSAR resolution. The current study developed the relationship between IRI and satellite data in terms of a mathematical model. Further study should be carried out to develop a physical properties model to explain this relationship.

Acknowledgements

References and Notes

1. Grote, K.; Hubbard, S.; Harvey J.; Rubin, Y. Evaluation of infiltration in layered pavements using surface GPR reflection techniques. *J. Appl. Geophys.* **2005**, *57*, 129-153.
2. Wang, H. *Road Profiler Performance Evaluation and Accuracy Criteria Analysis*; Virginia Polytechnic Institute and State University: Blacksburg, VA, USA, 2006; p. 73.
3. Sayers, M.W.; Karamihas, S.M. *The Little Book of Profiling—Basic Information about Measuring and Interpreting Road Profiles*; University of Michigan: Ann Arbor, MI, USA, 1998; p. 102.
4. Mactutis, J.A.; Alavi, S.H.; Ott, W.C. Investigation of relationship between roughness and pavement surface distress based on WesTrack project. *Transp. Res. Rec*. **2000**, *1699*, 107-113.
5. Baus, R.; Hong, W. *Investigation and Evaluation of Roadway Rideability Equipment and Specifications*; Report FHWA-SC-99-05; Federal Highway Administration/South Carolina Department of Transportation: Columbia, SC, USA, 1999.
6. Ksaibati, K.; McNamera, R.; Miley, W.; Armaghani, J. Pavement roughness data collection and utilization. *Transp. Res. Rec*. **1999**, *1655*, 86-92.
7. Kelly, L.S.; Leslie, T.G.; Lynn, D.E. *Pavement Smoothness Index Relationships: Final Report*; Publication No. FHWA-RD-02-057; Turner-Fairbank Highway Research Center, Federal Highway Administration, Research, Development, and Technology, U.S. Department of Transportation: McLean, VA, USA, 2002.
8. Benedetto, A.; Pensa, S. Indirect diagnosis of pavement structural damages using surface GPR reflection techniques. *J. Appl. Geophys.* **2007**, *62*, 107-123.
9. Dashevsky, Y.A.; Dashevsky, O.Y.; Filkovsky, M.I.; Synakh, V.S. Capacitance sounding: A new geophysical method for asphalt pavement quality evaluation. *J. Appl. Geophys.* **2005**, *57*, 95-106.
10. Simonsen, E.; Isacsson, U. Thaw weakening of pavement structures in cold regions. *Cold Reg. Sci. Technol.* **1999**, *29*, 135-151.
11. Terzi, S. Modeling the pavement serviceability ratio of flexible highway pavements by artificial neural networks. *Constr. Build. Mater.* **2007**, *21*, 590-593.
12. Bergmeister, K.; Santa, U. *Road Surface Monitoring and Pavement Analysis*; ASECAP: Pula, Croatia, 2006; pp. 283-288.
13. Saarenketo, T.; Scullion, T. Road evaluation with ground penetrating radar. *J. Appl. Geophys.* **2000**, *43*, 119-138.
14. Shresthaa, R.L.; Cartera, W.E.; Sartoria, M.; Luzuma, B.J.; Slatton, K.C. Airborne laser swath mapping: Quantifying changes in sandy beaches over time scales of weeks to years. *ISPRS J. Photogramm. Remote Sens.* **2005**, *59*, 222-232.
15. Alam, J.B.; Nahar, T.; Shaha, B. Evaluation of national highway by geographical information system. *Int. J. Environ. Res.* **2008**, *2*, 365-370.

16. Hans, Z.; Ryan, T.; Shauna, H.; Reg, S.; Sitansu, P. Use of LiDAR-Based elevation data for highway drainage analysis: A qualitative assessment. In *Proceedings of the 2003 Mid-Continent Transportation Research Symposium*, Ames, IA, USA, August 2003.

17. Stevens, L.B. *Road Surface Management for Local Governments—Resource Notebook*; Publication No. DOT-I-85-37; Federal Highway Administration: Washington, DC, USA, May 1985.

18. JAXA. Advanced land observing satellite website. Available online: http://www.alos-restec.jp/aboutalos_e.html (accessed on 15 May 2008).

19. Transportation Research Board (TRB). *Special Report 209: Highway Capacity Manual*, 3rd ed.; National Research Council: Washington, DC, USA, 2000.

20. DOH. Department of Highways, Thailand Website. Available online: http://www.doh.go.th/index_doh.aspx (accessed on 31 May 2007).

21. McFadden, D. Conditional logit analysis of qualitative choice behavior. In *Frontiers in Econometrics*; Zarembka, P., Ed.; Academic Press: New York, NY, USA, 1973.

Appendix

Table A1. Details of the PALSAR system [18].

Mode	Fine		ScanSAR	Polarimetric (Experimental mode)
Center Frequency	1270 MHz (L band)			
Chirp Bandwidth Polarization	28MHz HH or VV	14MHz HH+HV Or VV+VH	14MHz 28MHz HH or VV	14MHz HH+HV+VH+VV
Incident angle	8 to 60 °	18 to 43 °	18 to 43 °	8 to 30 °
Range Resolution	7 to 44 m	14 to 88 m	100 m (multi-look)	24 to 89 m
Observation Swath	40 to 70 km	40 to 70 km	250 to 350 km	20 to 65 km
Bit Length	5 bits	5 bits	5 bits	3 or 5 bits
Data rate	240 Mbps	240 Mbps	120 Mbps, 240 Mbps	240 Mbps
NE sigma zero	< −23 dB (swath width 70 km) < −25 dB (swath width 60 km)		< −25 dB	< −29 dB
S/A	< −16 dB (Swath width 70 km) < −21 dB (Swath width 60 km)		> 21 dB	> 19 dB
Radiometric accuracy	Scene: 1 dB / Orbit: 1.5 dB			

Table A2. Detailed information of the PALSAR sensor (Scene ID: ALPSRP067770280-P1.5GUA).

Item	Value
Operation Mode	PLR
Scene ID	ALPSRP067770280
Scene Shift	0
Pixel Spacing	12.5
Observation Path Number	483
Center Frame Number	280
Orbit Data	Precision
Image Scene Center Latitude, Longitude	14.449, 100.622
Image Scene Left Top Latitude, Longitude	14.714, 100.430
	(653603.184N, 1633021.952E)
Image Scene Right Top Latitude, Longitude	14.765, 100.692
Image Scene Left Bottom Latitude, Longitude	14.134, 100.552
Image Scene Right Bottom Latitude, Longitude	14.185, 100.814
Beginning Date of Observation (UTC)	2007/05/03 15:42:18
End Date of Observation (UTC)	2007/05/03 15:53:42
Total Orbit Number	6777
Sun Elevation	−53
Sun Azimuth	325
Source (Satellite) Code	AL
Orbit Direction	Ascending
Off-nadir (angle)	21.5
Table Number	127(−)
Reception Path Number	437
No Of Pixels (column)	3400
No Of Lines	5600
Process Level	1.5